ORIGINAL ARTICLE

Paracrine Activin-A Signaling Promotes Melanoma Growth and Metastasis through Immune Evasion

Prudence Donovan[1,4], Olivier A. Dubey[1,4], Susanna Kallioinen[1], Katherine W. Rogers[3], Katja Muehlethaler[2], Patrick Müller[3], Donata Rimoldi[2] and Daniel B. Constam[1]

The secreted growth factor Activin-A of the transforming growth factor β family and its receptors can promote or inhibit several cancer hallmarks including tumor cell proliferation and differentiation, vascularization, lymphangiogenesis and inflammation. However, a role in immune evasion and its relationship with tumor-induced muscle wasting and tumor vascularization, and the relative contributions of autocrine versus paracrine Activin signaling remain to be evaluated. To address this, we compared the effects of truncated soluble Activin receptor IIB as a ligand trap, or constitutively active mutant type IB receptor versus secreted Activin-A or the related ligand Nodal in mouse and human melanoma cell lines and tumor grafts. We found that although cell-autonomous receptor activation arrested tumor cell proliferation, Activin-A secretion stimulated melanoma cell dedifferentiation and tumor vascularization by functional blood vessels, and it increased primary and metastatic tumor burden and muscle wasting. Importantly, in mice with impaired adaptive immunity, the tumor-promoting effect of Activin-A was lost despite sustained vascularization and cachexia, suggesting that Activin-A promotes melanoma progression by inhibiting antitumor immunity. Paracrine Activin-A signaling emerges as a potential target for personalized therapies, both to reduce cachexia and to enhance the efficacy of immunotherapies.

Journal of Investigative Dermatology (2017) **137,** 2578–2587; doi:10.1016/j.jid.2017.07.845

INTRODUCTION

In melanoma research, targeted inhibitors and immune checkpoint therapies are available, but their efficacies remain limited by acquired and intrinsic drug resistance mechanisms (Lau et al., 2016). Patients with resistant melanoma have a poor prognosis due to high probability of metastasis, correlating with progression from superficial spreading to invasive vertical growth. Tumor-initiating potential and metastasis also correlate with low immunogenic profiles of subpopulations of cells and phenotypic plasticity marked by pseudoepithelial-to-mesenchymal transitions and the ability to reversibly switch between proliferative and invasive gene signatures (Caramel et al., 2013; Hoek et al., 2008; Schatton and Frank, 2009; Widmer et al., 2012). Thus, elucidating mechanisms of tumor immune evasion and their coupling to cancer cell plasticity is critical to develop effective immunotherapies.

Konstanzer Online-Publikations-System (KOPS)
URL: http://nbn-resolving.de/urn:nbn:de:bsz:352-2-ip4ge5btcxs33

[1]*Ecole Polytechnique Fédérale de Lausanne (EPFL) SV ISREC, Lausanne, Switzerland;* [2]*Centre Ludwig de l'UNIL pour la recherche sur le cancer, Epalinges, Switzerland; and* [3]*Friedrich Miescher Laboratory of the Max Planck Society, Tübingen, Germany*

[4]*These authors contributed equally to this work.*

Correspondence: Daniel B. Constam, Ecole Polytechnique Fédérale de Lausanne (EPFL) SV ISREC, Station 19, CH-1015 Lausanne, Switzerland. E-mail: Daniel.Constam@epfl.ch

Abbreviations: caALK4, constitutively active mutant Activin receptor-like kinase 4; FST, Follistatin; INHβA, Inhibin βA; TGFβ, transforming growth factor β

Received 16 January 2017; revised 26 June 2017; accepted 25 July 2017; accepted manuscript published online 26 August 2017

Known local cues in the tumor microenvironment that regulate melanoma cell plasticity and antitumor immunity include transforming growth factor β (TGFβ). In many tumors including melanoma, TGFβ facilitates or inhibits tumor progression, depending on the context (Bellomo et al., 2016; Perrot et al., 2013). In normal melanocytes, TGFβ induces cell cycle arrest and apoptosis (Alanko and Saksela, 2000; Rodeck et al., 1991), but this response is attenuated in cells from benign nevi despite sustained activation of downstream SMAD2,3 transcription factors (Rodeck et al., 1999). SMAD-binding sites in the *PAX3* gene mediating repression of pigment synthesis likely contribute to melanoma cell plasticity and phenotype switching (Pinner et al., 2009; Yang et al., 2008). TGFβ immunostaining was found to correlate with the invasive vertical growth phase and metastasis (Van Belle et al., 1996), and blockade of downstream SMAD2,3 transcription factors by overexpression of antagonistic SMAD7 in 1205Lu melanoma cells inhibited tumorigenicity and bone metastasis (Javelaud et al., 2005, 2007). In metastatic B16F10 mouse melanoma, TGFβ also reduces natural killer cell-mediated tumor rejection while promoting the differentiation of immunosuppressive Foxp3+ regulatory T cells in tumor beds and draining lymph nodes (Chen et al., 2003; Gorelik and Flavell, 2001; Turk et al., 2004). However, the functionally relevant active TGFβ in this model is provided by immature myeloid dendritic cells in draining lymph nodes, likely because B16F10 and other melanoma cells themselves secrete TGFβ only in latent form (Ghiringhelli et al., 2005; Yin et al., 2012).

Melanoma cell lines and tumors also frequently express Activin-A (Heinz et al., 2015; Hoek et al., 2006). Activin-A

© 2017 The Authors. Published by Elsevier, Inc. on behalf of the Society for Investigative Dermatology. This is an open access article under the CC BY license (http://creativecommons.org/licenses/by/4.0/).

stimulates the same SMAD transcription factors as TGFβ, even though it derives from distinct precursor dimers encoded by the *Inhibin βA* (*INHβA*) gene and binds distinct complexes of the Activin/Nodal type I and II receptors Acvr1b/ALK4 or Acvr1c/ALK7 and Acvr2 (reviewed in Hedger et al., 2011; Sozzani and Musso, 2011; Walton et al., 2011). Activin-A can mediate protective or tumorigenic effects (reviewed in Loomans and Andl, 2014). For example in mouse models of pancreatic cancer, Activin-A promotes tumor progression by inhibiting cell differentiation (Lonardo et al., 2011; Togashi et al., 2015). Paradoxically, its receptor ALK4 (ACVR1B) primarily mediates tumor suppressive functions and is frequently deleted in clinical samples (Qiu et al., 2016; Togashi et al., 2014). Cytostatic and proapoptotic signaling by Activin-A has also been reported in human melanoma cell lines, although this activity is counteracted by the secreted antagonist Follistatin (FST-1) (Stove et al., 2004). Immunohistochemical analysis detected Activin-A staining in superficially spreading melanoma, whereas benign nevi and metastatic lesions showed elevated expression of FST (Heinz et al., 2015). Interestingly, however, gain of transgenic Activin-A expression in the A375 human melanoma xenograft model did not alter tumor growth or metastasis, even though it reduced tumor lymphangiogenesis, a risk factor of poor prognosis (Heinz et al., 2015). Also in xenograft models of other cancers, overexpression of a dominant negative mutant receptor revealed no adverse functions for Activin-A or related ligands, with the exception of tumor-induced systemic weight loss (cachexia) through remote Smad2,3 activation in skeletal muscles (Li et al., 2007; Zhou et al., 2010).

Here, we asked whether a potential tumorigenic role for Activin signaling in melanoma may be curtailed in xenografts by the absence of a functional immune system. To address this, we monitored the expression of *INHβA* in public datasets and in a panel of melanoma tumors and cell lines, and we performed loss- and gain-of-function studies, respectively, in human xenografts and in the moderately metastatic syngeneic B16F1 mouse melanoma model using dominant negative or ligand-independent mutant Activin/Nodal receptors or Activin-A lentiviral transgenes. Our comparison of melanoma grafts in tumor hosts of different genetic backgrounds reveals a protumorigenic and prometastatic function specifically for paracrine Activin-A signaling acting on adaptive immunity, and that this function can be uncoupled from immune-independent anorexic and proangiogenic effects and from autocrine effects on melanoma cell differentiation. Our findings suggest that gain of Activin-A expression in human melanoma should be considered as a potential target for improved immunotherapies.

RESULTS

Human melanoma and other skin cancers frequently express Activin-A rather than NODAL

To assess potential roles of *INHβA* in melanoma, we queried a gene expression profiling dataset of 42 primary cutaneous tumors (Riker et al., 2008). We found that *INHβA* expression was significantly elevated both in primary cutaneous cancers and in metastatic melanoma, whereas the antagonist FST tended to decrease in melanoma in situ ($n = 2$, not significant) compared with normal skin. In contrast to *INHβA*, other Activin receptor ligands encoded by *NODAL* or *GDF3* were neither upregulated in this dataset nor in a TCGA collection of 474 skin cutaneous melanomas (Figure 1a, Supplementary Figure S1 online). Elevated *INHβA* expression significantly clustered with a standard gene expression signature of invasive rather than proliferative melanoma cell lines as determined by Heuristic Online Phenotype Prediction analysis (Figure 1b) (Widmer et al., 2012). Furthermore, although RT-PCR analysis confirmed *INHβA* expression in more than half of a panel of 20 human melanoma cell lines, the related ligands encoded by *INHβB* or *NODAL* were rarely transcribed or undetectable, respectively (Figure 1c, Supplementary Figure S2 online). Although survival did not correlate with either *INHβA* or *NODAL*, low expression of the Activin antagonist *Follistatin* in the TCGA dataset was associated with worse outcome (Supplementary Figure S3 online). These results are consistent with a potential role for Activin-A signaling in melanoma progression.

Inhibition of endogenous ActRIIB ligands in human C8161 melanoma cells inhibits cachexia but not tumor progression in immunocompromised nude mice

Previous analysis of Activin-A functions in tumor xenograft models uncovered potent anorexic activity but no important roles in tumor progression (Heinz et al., 2015; Zhou et al., 2010). Instead, increased aggressiveness in human melanoma has been attributed to a secreted Nodal-like activity that was initially detected by injecting C8161 melanoma cells into zebrafish embryos (Topczewska et al., 2006). Because we observed no *NODAL* expression in human melanoma, we decided to reassess how C8161 cells stimulate Nodal/Activin receptors in zebrafish. To address this, we grafted C8161 cells into wild-type or mutant zebrafish embryos lacking maternal and zygotic expression of the Nodal coreceptor *one-eyed pinhead* (MZ*oep*) (Gritsman et al., 1999). To validate that human NODAL signaling requires Oep in zebrafish, we injected 50 pg of mRNA encoding human Nodal at the one-cell stage and monitored induction of the Smad2,3 target gene *gsc* during early gastrulation. We found that both human Nodal and the zebrafish homolog Squint were active in wild-type but not in MZ*oep*, whereas human Activin-A induced *gsc* independently of Oep (Supplementary Figure S4a online). Moreover, both wild-type and MZ*oep* embryos ectopically upregulated *gsc* as well as *ntl* around grafted C8161 melanoma cells (Supplementary Figure S4b). These results strongly argue for secreted Activin-A and against Nodal as the mediator of Smad2,3 signaling secreted by C8161 melanoma grafts in zebrafish.

To test whether melanoma may grow faster when forced to express Nodal, C8161 cells transduced with Nodal lentivirus (Supplementary Figure S2d) were grafted subcutaneously into FoxN1$^{nu/nu}$ mice. C8161 xenograft tumor growth was not increased by Nodal compared with cells transduced with empty vector, indicating that it was not limited by the lack of Nodal expression (Supplementary Figure S4e and f). To assess the function of endogenous ligands in melanoma xenografts, we transduced human C8161 cells with lentivirus expressing an Fc fusion of Activin type IIB receptor extracellular domain (AIIB-Fc) or Fc alone. Lentivirally transduced AIIB-Fc inhibited

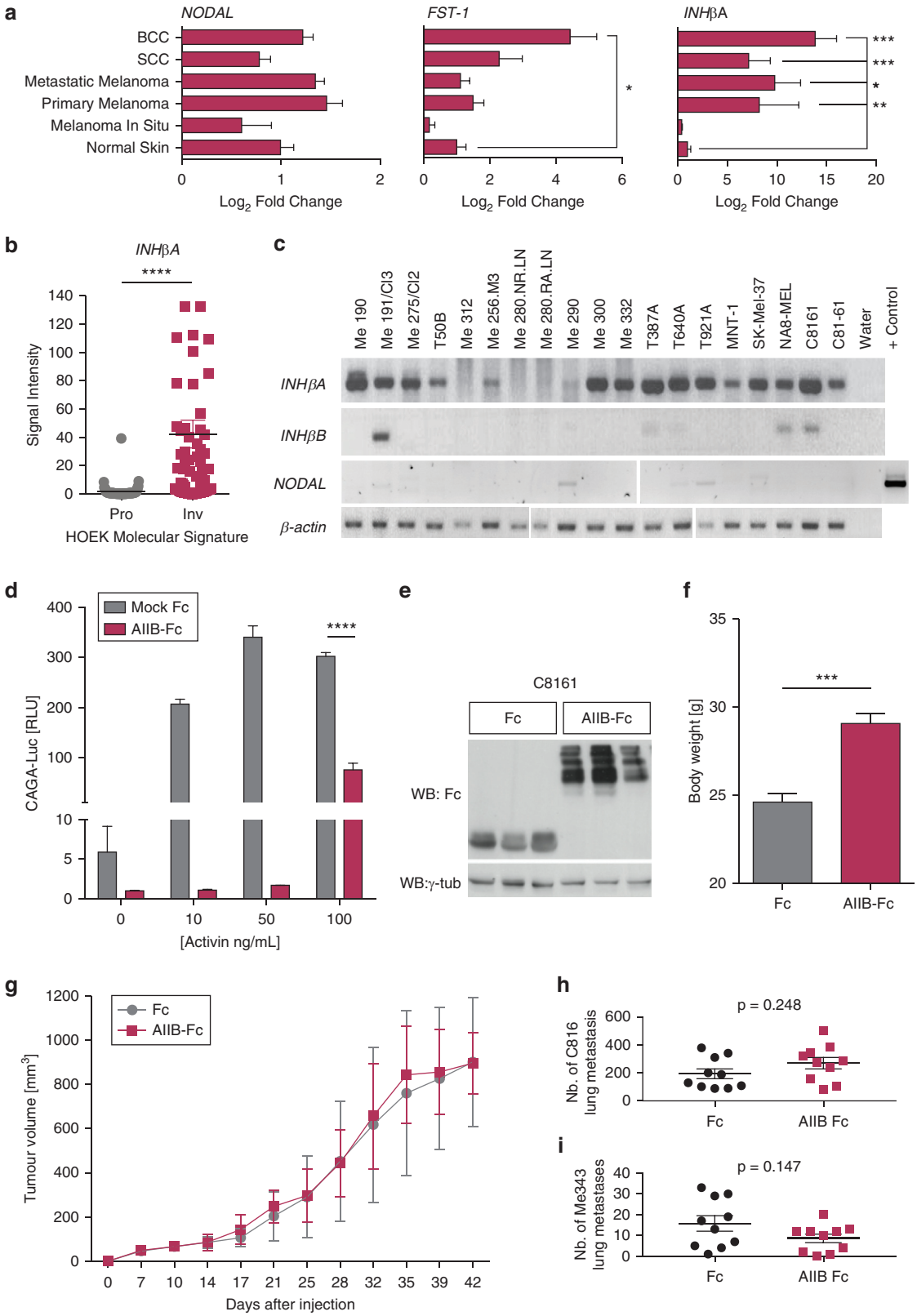

Figure 1. Cachexia induced by endogenous Activin-A in human melanoma xenografts does not promote tumor progression. (**a**) Expression of *NODAL*, Follistatin (*FST-1*), and *INHβA* (encoding Activin-A) mRNAs in normal skin compared with 42 primary cutaneous tumors comprising 14 melanoma, 11 squamous cell, 15 basal cell skin cancers, and 40 melanoma metastases (Riker et al., 2008). $^{*}P < 0.05$; $^{**}P < 0.01$; $^{***}P < 0.001$. (**b**) Relative *INHβA* mRNA levels in 536 human melanoma cell lines distinguished by proliferative (Pro) or invasive (Inv) gene expression signatures (Widmer et al., 2012). $^{****}P < 0.0001$. (**c**) RT-PCR analysis of the indicated mRNAs in total RNA from human melanoma cell lines or fetal brain (+Control). (**d**) Normalized expression of the Smad3 luciferase reporter CAGA-Luc in HEK293T cells treated with the indicated concentration of Activin-A or with conditioned media of C8161 melanoma cells expressing lentiviral AIIB-Fc or Fc alone (mock). Data show the average fold change of three experiments ± SD, $^{****}P < 0.0001$ at all concentrations.

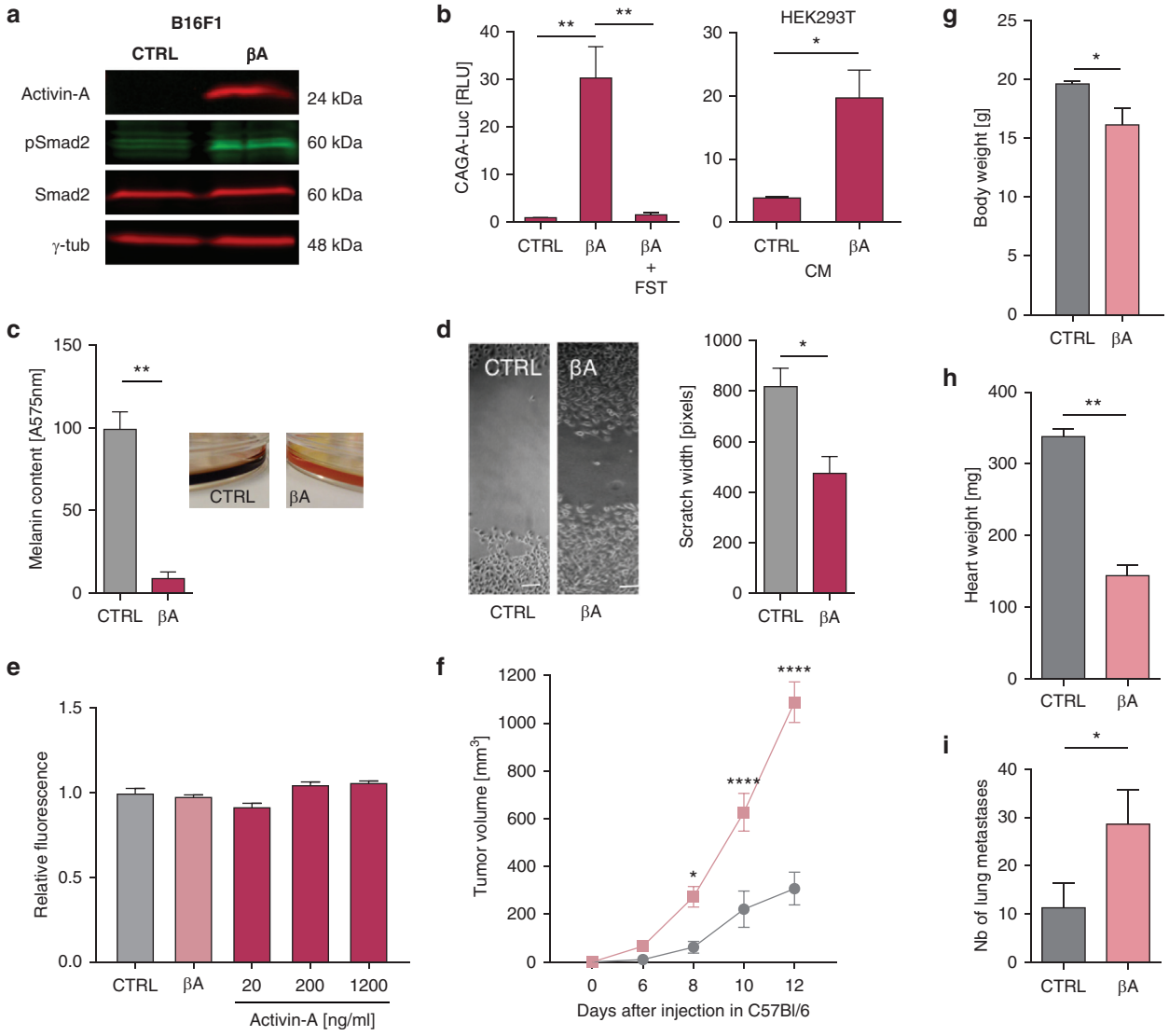

Figure 2. Gain of Activin-A expression stimulates phenotype switching and syngeneic tumor growth in B16F1 mouse melanoma. (**a**) Western blot of secreted Activin-A and (**b**) CAGA-Luc expression in B16F1:GFP cells (left panel) transduced with *INHβA* (βA) or control lentivirus (CTRL). Where indicated, cells were treated with Follistatin (FST, 300 ng/ml). CAGA-Luc expression in HEK293T cells treated with conditioned media of B16:GFP.βA or B16:GFP.CTRL cells is also shown (right panel in **b**). Data represent mean ± SEM of three experiments; $*P < 0.05$, $**P < 0.01$. (**c**) Light absorbance by pigment in medium of transduced B16F1:GFP cells (mean ± SEM, n = 3; $**P < 0.01$). (**d**) Representative micrographs and widths of scratch wounds 20 hours after wounding of cell monolayers (mean ± SEM from three experiments, $*P < 0.05$). (**e**) Alamar blue quantification of live B16F1 cells transduced with control or *INHβA* lentivirus, or treated with the indicated concentrations of Activin-A for 48 hours (mean ± SEM, n = 3, no significant differences). (**f**) Growth curves of B16F1:GFP syngeneic intradermal grafts with Activin-A (βA) or without (CTRL) in C57BL/6 mice, and (**g**) body and (**h**) heart weights at the time of tumor resection. Data represent mean ± SEM of 20 animals/group; $*P < 0.05$, $**P < 0.01$, $****P < 0.0001$. (**i**) Lung metastases of tail-vein injected B16F1:GFP βA or CTRL cells (n = 15 each). Data represent mean ± SEM of three experiments; $*P < 0.05$. GFP, green fluorescent protein; INHβA, Inhibin βA; SEM, standard error on the mean.

endogenous Activin activity in the conditioned medium of C8161 cells in vitro and was readily detected by immunoblotting in C8161 tumor xenografts (Figure 1d and e). As expected, expression of AIIB-Fc in C8161 xenografts significantly protected FoxN1$^{nu/nu}$ hosts against loss of body weight and muscle mass (Figure 1f). However, despite potent systemic inhibition of cachexia, soluble AIIB-Fc receptor neither diminished intradermal tumor growth nor experimental lung metastases after tail vein injection (Figure 1g and h). Additionally, secondary tumor outgrowths after resection of the primary C8161 graft and spontaneous lung or lymph node metastases were not significantly inhibited (Supplementary Figure S5a–c online), nor did AIIB-Fc transduction inhibit experimental lung metastases of

(**e**) Western blot analysis of lentiviral AIIB-Fc or Fc alone in intradermal C8161 melanoma xenograft tumors, and (**f**) body weights of Foxn1nu/nu hosts at the time of tumor resection ($***P < 0.01$). (**g**) Growth curves of C8161 melanoma were unaffected by AIIB-Fc expression. (**h**) Number of superficial lung metastases of C8161-Fc (MockFc) or C8161-AIIBFc melanoma cells 4 weeks after injection into the tail vein of Foxn1$^{nu/nu}$ mice (n = 10 per group, $P = 0.25$, two-tailed Mann-Whitney). (**i**) As in (**h**), but using human Me343 melanoma cells (n = 10 per group, $P = 0.14$). INHβA, Inhibin βA; SD, standard deviation.

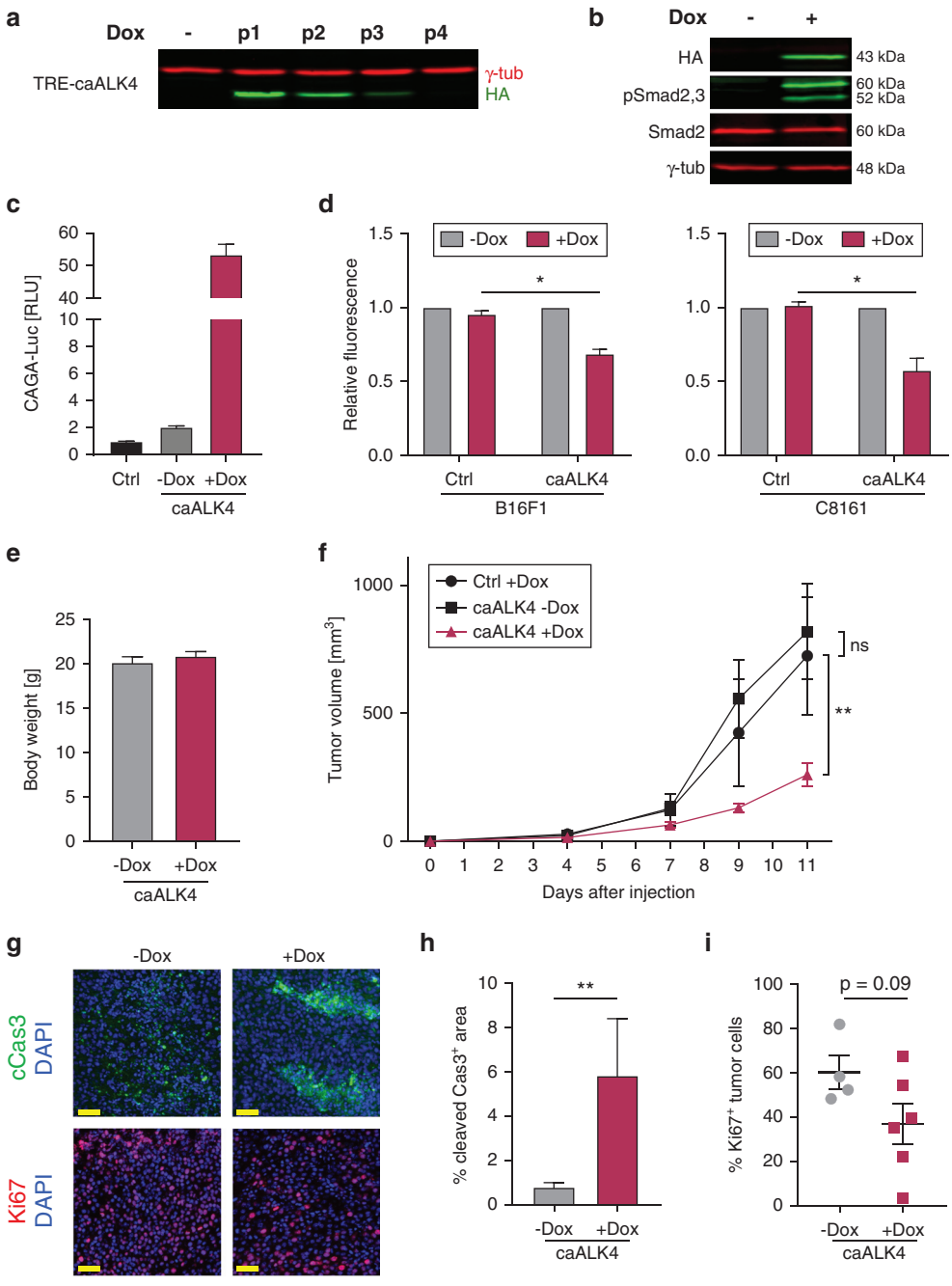

Figure 3. Sustained autocrine Activin receptor signaling inhibits B16F1 cell survival and tumorigenesis rather than stimulating it. (**a, b**) Anti-HA and phospho-Smad2,3 Western blot of B16F1 cells treated with doxycycline during (**a**) 4 cell passages or (**b**) 24 hours after lentiviral infection of inducible HA-tagged caALK4 (rtTA-caALK4). (**c**) CAGA-Luc expression in B16F1 (Ctrl) or B16F1 rtTA-caALK4 cells ± doxycycline for 24 hours. Data represent mean ± SEM of three experiments. (**d**) Alamar blue assay of B16F1 or C8161 (Ctrl) and B16F1 rtTA-caALK4 or C8161 rtTA-caALK4 cells cultured for 3 days in medium with or without doxycycline. Data represent mean ± SEM of two experiments, $*P < 0.05$. (**e**) Body weights of C57BL/6 hosts at the time of tumor resection after feeding with or without doxycycline, and (**f**) growth curves of intradermal syngeneic grafts of B16F1 rtTA (Ctrl, n = 15) and B16F1 rtTA-caALK4 cells (n = 15). Data represent mean ± SEM of three experiments, $**P < 0.01$. (**g**) Cleaved Caspase-3 (cCas3) and Ki67 immunofluorescence staining of syngeneic B16F1 tumors expressing caALK4 (+Dox) or not (−Dox). Scale bar: 50 μm. Corresponding whole-section images are shown in Supplementary Figure S7f. (**h**) Quantification of cCas3+ area from entire sections revealed increased apoptotic areas in +Dox (n = 6) compared with −Dox tumors (n = 5), $**P < 0.01$. (**i**) Flow cytometry of proliferative (Ki67+) cells in syngeneic B16F1 tumors expressing caALK4 (+Dox) or not (−Dox). A trend for decreased proliferation in caALK4 tumors (n = 6) compared with controls (n = 4) was not significant ($P = 0.09$). caALK4, constitutively active mutant Activin receptor-like kinase 4; Dox: doxycycline; HA, human influenza hemagglutinin; SEM, standard error on the mean.

Me343 cells that also express *INHβA* (Figure 1i, Supplementary Figure S2g). These results suggest that C8161 xenografts grow and metastasize independently of Activin signaling and of associated systemic cachexia, possibly because of the lack of functional adaptive immunity.

Activin-A gain of function promotes phenotype switching of mouse melanoma cells and tumor progression

To evaluate potential tumorigenic or prometastatic effects of Activin-A in immunocompetent hosts, we transduced *INHβA* in the moderately metastatic syngeneic B16F1 mouse melanoma model (Fidler, 1973) using lentiviruses for green fluorescent protein alone (CTRL) or green fluorescent protein together with Activin-A (INHβA). Western blot analysis of B16F1-conditioned medium and cell lysates confirmed Activin-A secretion that increased the accumulation of pSmad2 compared with CTRL cells that do not secrete Activin-A (Figure 2a). Transfection of the SMAD3 luciferase reporter CAGA-Luc showed elevated autocrine Activin-A signaling in *INHβA*- compared with CTRL-transduced B16F1 cells, and this increase was blocked on treatment with FST (Figure 2b, left panel). Conditioned medium from *INHβA*-transduced B16F1 cells also stimulated the expression of transfected CAGA-Luc in HEK293T reporter cells (Figure 2b, right panel). Furthermore, gain of Activin-A expression in B16F1 cells stimulated their migration in a scratch wound assay and markedly reduced their melanin content without altering their cell proliferation or viability (Figure 2c–e),

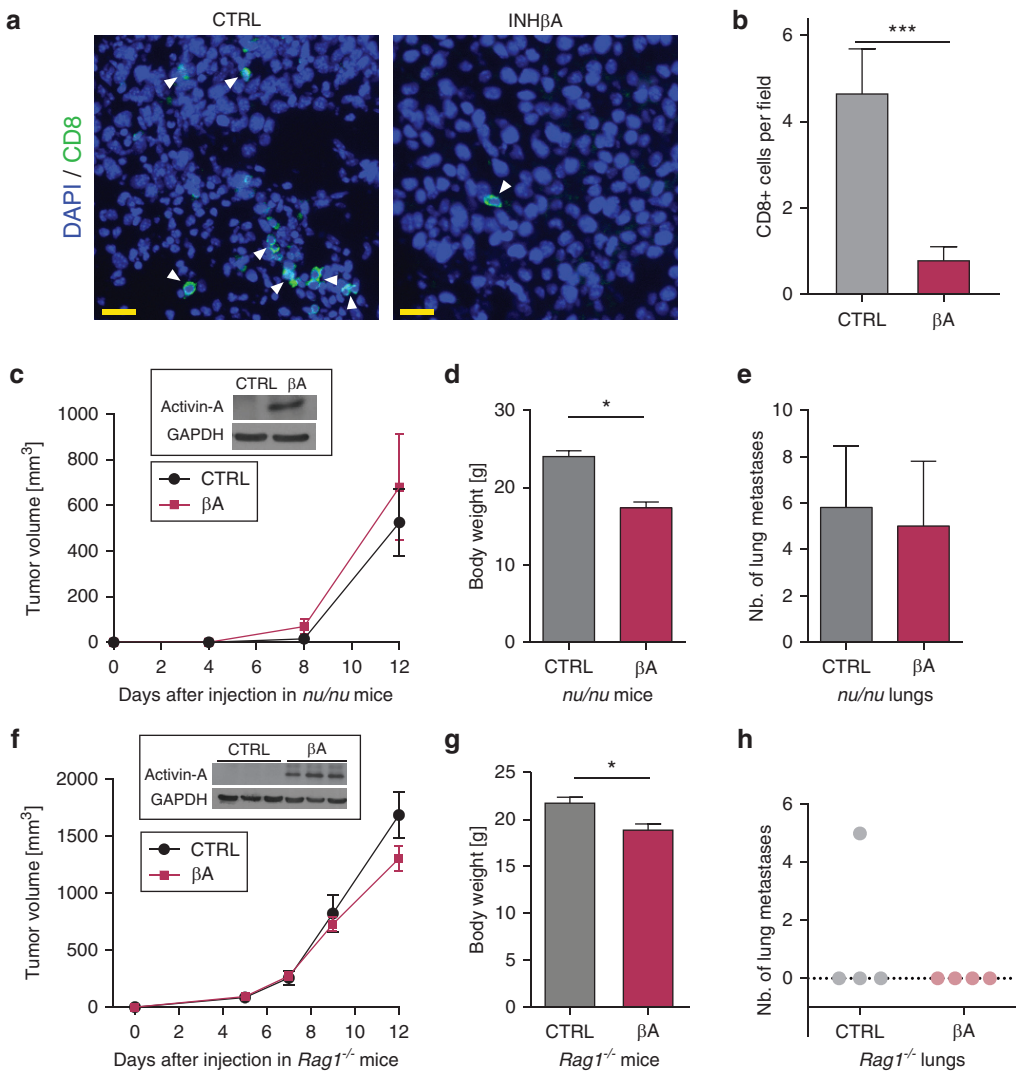

Figure 4. Tumorigenic activity of paracrine Activin-A signaling is mediated by the adaptive immune system. (**a**) CD8 immunostaining (green) of B16F1:GFP CTRL (n = 4) or βA (n = 3) syngeneic intradermal grafts counterstained with DAPI (blue). Arrowheads point to cells positive for CD8 staining. Scale bars: 25 μm. (**b**) Quantification of tumor-infiltrating lymphocytes (mean ± SEM, ***$P <$ 0.001). Cells positive for CD8 staining were counted in 1,000 pixel-wide fields. (**c**) Growth curves of CTRL or βA-expressing B16F1:GFP tumors (n = 5 each) after intradermal injection in the right flank of Foxn1$^{nu/nu}$ mice. Inset: Western blot of Activin-A in randomly chosen tumor extracts at the experimental endpoint. GAPDH served as loading control. (**d**) Body weights of the hosts of the tumors shown in (a) (mean ± SEM, *$P < 0.05$). (**e**) Experimental lung metastases observed after tail vein injection of CTRL or βA-expressing B16F1:GFP (n = 10 each) in Foxn1$^{nu/nu}$ mice. (**f**) Volumes of intradermal CTRL- (n = 4) or βA-B16F1:GFP tumor grafts (n = 3) in the right flank of *Rag1*$^{-/-}$ mice. Western blots were as in panel (**a**). (**g**) Body weight at the time of tumor resection. *Rag1*$^{-/-}$ mice injected with βA expressing B16F1:GFP develop cachexia (n = 4) compared with CTRL injected animals (n = 4). Data represent mean ± SEM; *$P < 0.05$. (**h**) Numbers of experimental lung metastases after tail vein injection of B16F1:GFP ± CTRL (n = 4) or βA (n = 4) in *Rag1*$^{-/-}$ mice. GAPDH, glyceraldehyde-3-phosphate dehydrogenase, GFP, green fluorescent protein; INHβA, Inhibin βA; SEM, standard error on the mean.

consistent with a potential autocrine function in promoting a phenotypic switch.

To determine if the oncogenic effects of Activin-A gain of function may promote tumor growth in vivo, B16F1 grafts were intradermally inoculated on the right flank of 8- to 10-week-old female C57BL/6 mice. Mice injected with *INHβA*-transduced cells grew significantly larger tumors, combined with loss of body weight and cardiac muscle wasting (Figure 2f–h). Compared with vector control, *INHβA* also increased the number of experimental lung metastases formed by tumor cells that were injected into the tail vein (Figure 2i). Taken together, these results show that Activin-A signaling can promote melanoma growth and metastasis in immunocompetent hosts.

Sustained cell autonomous ALK4 signaling inhibits B16F1 tumorigenesis rather than stimulating it

To validate whether the tumorigenic function of Activin-A involves cell nonautonomous paracrine signaling, we transduced B16F1 cells with lentivirus expressing a constitutively active ligand-independent truncated form of ALK4 (caALK4). Induction of caALK4 by doxycycline led to increased Smad2,3 phosphorylation and expression of the SMAD3-dependent luciferase reporter CAGA-Luc (Figure 3a–c) and reduced pigment secretion (Supplementary Figure S6a online). However, caALK4 expression decreased below detection within four subsequent cell passages despite the continuous presence of doxycycline (Figure 3a). 5-ethynyl-2′-deoxyuridine incorporation, AnnexinV and propidium iodide flow cytometry, and cleaved Caspase3 immunofluorescence staining after up to 3 days of caALK4 induction in vitro revealed no overt cell cycle inhibition or apoptosis (Supplementary Figure S7a–d online and data not shown), even though the number of cells detected by Alamar blue assays after 3 days of caALK4 induction *in vitro* was reduced (Figure 3d), indicating impaired cell viability. A similar reduction in the number of viable cells was induced by ligand-independent caALK4 in human C8161 melanoma cells. To investigate the impact on tumor growth, B16F1 cells transduced with caALK4 were grafted intradermally into

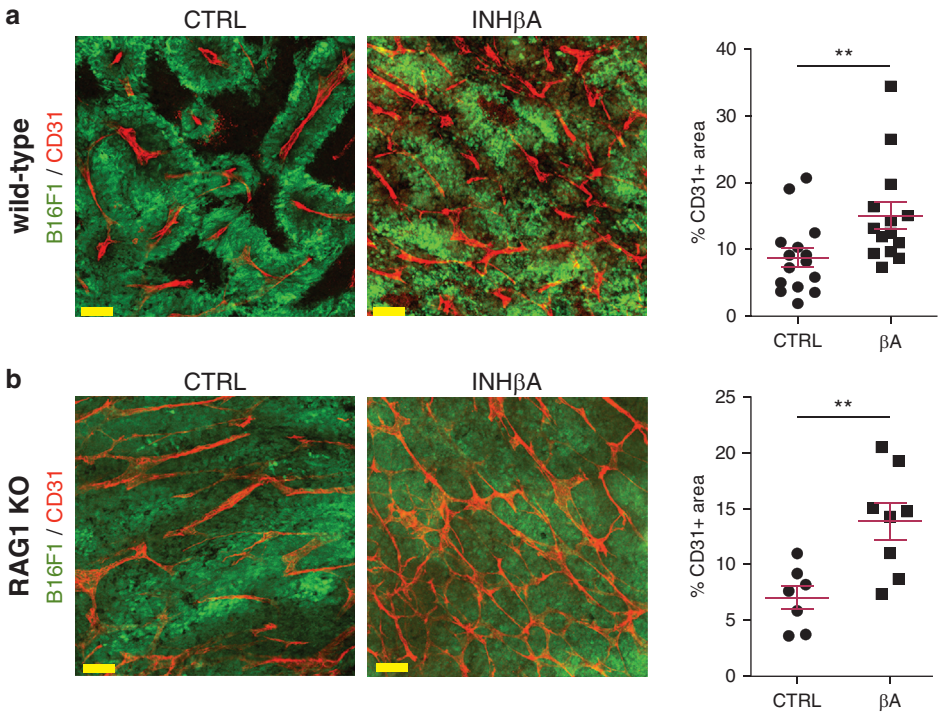

Figure 5. Paracrine Activin-A can stimulate tumor angiogenesis and oxygenation independently of adaptive immunity. CD31 immunofluorescence staining (red) of thick sections of B16F1:GFP CTRL or βA syngeneic intradermal grafts (green) in wild-type and *Rag1*$^{-/-}$ C57BL/6 mice. Quantifications (right panels) show that βA-expressing tumors had significantly increased vascular coverage compared with CTRL tumors both in wild-type (βA: n = 14; CTRL: n = 15) and in *Rag1*$^{-/-}$ hosts (βA: n = 8; CTRL: n = 7). $^{**}P < 0.01$. GFP, green fluorescent protein; INHβA, Inhibin βA.

syngeneic C57BL/6 hosts, followed by treatment with doxycycline or empty vehicle until the endpoint of the experiment. Tumors induced no overt loss of body weight (Figure 3e), and they grew significantly less in doxycycline-fed animals than in vehicle-treated controls (Figure 3f), indicating that sustained autocrine Activin receptor signaling does not stimulate but rather suppresses tumor growth in vivo. Immunostaining at the endpoint of the experiment revealed increased apoptosis marked by cleaved Caspase-3 (Figure 3g, Supplementary Figure S7e), whereas Ki67-stained proliferating cells appeared to decrease, albeit not significantly (Figure 3h and i, Supplementary Figure S7f). We conclude that whereas paracrine functions of Activin-A promote cachexia and tumor growth, sustained autocrine receptor signaling in vivo reduces B16F1 cell survival and tumorigenicity.

Activin-A-dependent B16F1 melanoma growth is mediated by impaired tumor immune surveillance

One possible mechanism how paracrine Activin-A signaling accelerates tumor growth is by inhibiting tumor immune surveillance. In keeping with this idea, immunostaining of tumor sections with anti-CD8 antibody revealed that Activin-A expression significantly inhibited tumor infiltration by cytotoxic T-lymphocytes (Figure 4a and b). To directly test whether paracrine Activin-A signaling promotes tumor progression by inhibiting antitumor immunity, B16F1 cells were inoculated subcutaneously or intravenously into FoxN1$^{nu/nu}$ that lack functional T cells, or into *Rag1*$^{-/-}$ mice devoid of V-D-J recombination in antigen receptors. In sharp contrast to immune-competent wild-type hosts, loss of either *FoxN1* or *Rag1* enabled CTRL tumors to grow as fast as those with sustained *INHβA* expression, even though Activin-A provoked cachexia irrespective of the host genotype (Figure 4a–f). In good agreement, the same lentiviral *INHβA* transgene also failed to stimulate tumor growth or experimental lung metastases in xenografts of human melanoma cell lines in immunodeficient FoxN1$^{nu/nu}$ mice (Supplementary Figure S5d–g). These results strongly suggest that Activin-A accelerates B16F1 melanoma growth by blunting T-cell-mediated antitumor immunity.

Angiogenesis is enhanced by Activin-A but is not sufficient to promote B16F1 melanoma growth

Depending on the context, Activin-A signaling may also promote or inhibit angiogenesis that can be rate-limiting for tumor oxygenation and nutrient supply (Lewis et al., 2016). To assess whether increased tumor growth correlates with increased tumor vascularization, we labeled blood vessels in thick cryosections of syngeneic B16F1 grafts using CD31 antibodies. Quantification in z-stack reconstructions of entire sections of 15 CTRL and 14 INHβA tumors showed that Activin-A significantly increased the vascular density (Figure 5a). Conversely, pimonidazole staining of hypoxic areas in the same sections was 4-fold reduced, indicating that Activin-induced blood vessels were functional (Supplementary Figure S8a and b online). Because Activin-A has been shown to inhibit endothelial cell growth and tubule formation in vitro (Kaneda et al., 2011), we asked whether its proangiogenic effect in B16F1 melanoma could be mediated by macrophages. However, FACS sorting of dissociated B16F1 melanoma at the experimental endpoint revealed no changes in total myeloid populations, and M2-like macrophages marked by CD206 staining were decreased in *INHβA* compared with CTRL tumors (Supplementary Figure S8c). Also in human melanoma with the highest levels of Activin-A, markers of lymphocytic or myeloid infiltrates appeared to be reduced rather than increased (Supplementary Figure S9 online), although recruitment of such infiltrates or their functions may vary depending on Activin-A

signaling strength or duration. Interestingly, angiogenesis was similarly increased in *Rag1*$^{-/-}$ hosts where tumor growth remained unchanged on *INHβA* overexpression, suggesting that increased vascularization alone cannot account for the tumorigenic effects of Activin-A (Figure 5b).

DISCUSSION

Previous studies reported both tumor-suppressive and oncogenic effects of Activin-A, but a role in antitumor immunity and the relative contributions of autocrine versus paracrine signaling in an in vivo model of melanoma remained to be evaluated. Here, we propose that the net outcome of a gain in paracrine Activin-A signaling in mouse and human melanoma grafts is determined by whether or not the tumor host has functional adaptive immunity. Tumorigenic paracrine effects on adaptive immunity trumped proapoptotic autocrine signals within cancer cells to overall facilitate primary and metastatic growth. Ectopic Activin-A signaling also stimulated tumor vascularization and, concurring with previous reports, systemic cachexia, and these effects were preserved in *Rag1*$^{-/-}$ mice albeit without accelerating tumor growth. Thus, a potential boost in nutrient supply by recycled tissue breakdown products was either insufficient to fuel tumorigenesis or neutralized by growth-inhibitory autocrine Activin receptor signaling within tumor cells. To our knowledge, these results furnish direct evidence that adaptive immunity is required for a tumorigenic Activin function, and that autocrine and paracrine signaling mediates opposite effects on melanoma growth in vivo. Based on these findings, future strategies to boost the efficacy of immunotherapies should consider targeting Activin-A.

Activin-A only stimulates melanoma growth in mice that have functional T cells

Our main finding is that paracrine Activin-A signaling was tumorigenic specifically in immunocompetent hosts, despite a proapoptotic function of autocrine Activin/Nodal receptor signaling within melanoma cells. Thus, a lentiviral *INHβA* transgene encoding secreted Activin-A in syngeneic B16F1 mouse melanoma grafts increased intradermal tumor growth and the frequency of experimental lung metastases specifically in wild-type C57BL/6 mice. By contrast, in syngeneic *Rag1*$^{-/-}$ hosts that lack T- and B-lymphocytes, or in athymic *FoxN1*$^{nu/nu}$ mice devoid of only T cells, neither blockade of endogenous Activin/Nodal receptor ligands in the human C8161 melanoma cell line nor overexpression of Activin-A revealed a tumorigenic function. Technical artifacts arising from clonal variation or specific cell lines are unlikely because we used nonclonal pools of lentivirally transduced cells, and reproducible results were obtained with multiple independent batches of cells and with additional human melanoma cell lines. In keeping with our observations, also other tumor types in immunocompromised mice revealed minimal or no oncogenic effects of Activin-A (Zhou et al., 2010). Notable exceptions are pancreatic and esophageal cancer and R30C mammary carcinoma cells where gain of autocrine Activin signaling directly stimulates tumor cell stemness or survival (Krneta et al., 2006; Lonardo et al., 2011).

Induction of metastatic disease in chemically induced squamous cell carcinoma by a keratinocyte-specific *INHβA* transgene facilitates infiltration by immunosuppressive Tregs while reducing the number of resident γδ-TCR-positive dendritic epidermal T-lymphocytes, consistent with a potential role in promoting immune evasion (Antsiferova et al., 2011). Depletion of CD4-positive T cells, including Tregs, did not suppress the tumorigenicity of transgenic Activin-A in this skin carcinoma model (Antsiferova et al., 2017). However, it will be interesting to compare in future studies the potential of Tregs or tumor-infiltrating cytotoxic T-lymphocytes or other T-cell subsets to mediate effects of Activin-A on antitumor immunity in melanoma. A role in suppressing antitumor immunity may explain why *INHβA* expression is more frequently upregulated in human melanoma and other solid human tumors than expected for a neutral bystander (Hoda et al., 2016; Wu et al., 2015).

Inhibition of melanoma growth by autocrine signaling may curtail oncogenic effects of secreted Activin-A on the tumor microenvironment

We found that in contrast to secreted Activin-A, autocrine signaling by a doxycycline-inducible ligand-independent mutant ALK4 transgene inhibited B16F1 tumor growth rather than stimulating it. This confirms that oncogenic Activin-A activity in immunocompetent syngeneic hosts was mediated by paracrine signaling. Induction of caALK4 also inhibited the expansion of cultured B16F1 cells ex vivo. Although we cannot rule out that forced ALK4 signaling may induce non-physiological levels of Smad2/3 phosphorylation, cell proliferation and survival are also inhibited in normal melanocytes treated with Activin-A. By contrast, Activin-A-treated B16F1 cells proliferated normally. Because melanoma cell survival was impaired by caALK4 but not by secreted Activin-A, autocrine signaling activity of the ligand is likely attenuated in transformed cells compared with normal melanocytes. In the hepatocyte lineage, autocrine antiproliferative Activin-A signaling is frequently attenuated by secreted antagonists in hepatocarcinoma (reviewed in Deli et al., 2008). Also in human melanoma, dynamic changes in the levels of FST expression during progression of melanoma in situ to metastatic growth may modulate Activin-A responses (Heinz et al., 2015; Stove et al., 2004). However, whether FST influences the balance between autocrine and paracrine Activin signaling remains to be determined.

Interplay of tumor growth and cachexia

Commonly associated with advanced cancer in human patients, cachexia reduces life quality and drug responses while increasing morbidity and mortality (Fearon et al., 2013). In pancreatic MIA PaCa-2 xenografts, a comparison of tumor growth with the time course of Activin-induced cachexia suggests that associated metabolic changes or general weakening curtails a growth-promoting effect of autocrine Activin signaling (Togashi et al., 2015). If cachexia similarly curbs the growth of B16F1 melanoma growth, tumor growth should slow down concurring with the onset of Activin-induced cachexia at least in immunodeficient hosts. Such a trend in *Rag1*$^{-/-}$ hosts was not statistically significant and not seen in *nu/nu* hosts. The observed tumor growth curves also do not support a model that cachexia is rate-limiting for the supply of essential amino acids and other metabolites to cancer cells in a process of "autocannibalism" (Theologides, 1979).

Activin-induced tumor angiogenesis and its uncoupling from tumor growth

We found that paracrine Activin-A signaling in the syngeneic B16F1 melanoma model also stimulated tumor vascularization. However, a similar increase of blood vessels in *Rag1*$^{-/-}$ hosts was not sufficient to facilitate tumor growth. Although we could not stain enough tumors in *Rag1*$^{-/-}$ mice with pimonidazole to formally exclude a stimulatory effect of adaptive immunity on vessel functionality and hypoxia, it is interesting to note that tumor growth was also uncoupled from angiogenesis in immunodeficient SCID mice bearing mammary carcinoma xenografts, where gain of Activin-A signaling diminished tumor angiogenesis without affecting vascular perfusion (Krneta et al., 2006). Interestingly, however, Activin signaling within endothelial cells in this breast cancer model and other tumors was cytostatic and reduced sprouting and blood vessel density (Breit et al., 2000; Kaneda et al., 2011; Krneta et al., 2006), indicating that proangiogenic activity is likely indirect. T-cell-derived cytokines are unlikely involved because Activin-A stimulated the vascularization of B16F1 tumors even in *Rag1*$^{-/-}$ syngeneic hosts. Possibly, class I inflammatory macrophages that stimulate vascularization in Activin-induced skin squamous cell carcinoma mediate proangiogenic activity (Antsiferova et al., 2017). Although the total number of infiltrating macrophages was unchanged by Activin-A in B16F1 melanoma under the conditions examined, and because increased angiogenesis was not sufficient to promote tumor growth, we did not further investigate whether Activin-A directly polarized a proangiogenic macrophage subtype in this model.

Overall, our findings suggest that paracrine Activin-A should be considered as a target for personalized therapies not only to reduce cachexia and melanoma vascularization, but also to enhance the efficacy of immunotherapies.

MATERIALS AND METHODS

Melanoma grafts

A total of 1×10^6 B16F1 cells were injected intradermally into the right flank of 8- to 12-week-old female wild-type (Harlan) or *Rag1*$^{-/-}$ C57BL/6 (EPFL animal core facility) syngeneic hosts, or of Hsd-athymic *nu/nu* mice (Harlan). Animal body weights and tumor sizes were measured every 2 days. Tumor volumes were calculated using the formula *length* × *width* × *depth*. Experimental lung metastases were obtained by injecting 3×10^5 B16F1 cells into the tail vein. Pigmented metastases visible at the surface of each lung lobe were counted 3 weeks after injection. Where indicated, animals were fed with chow containing 0.625 g/kg doxycycline (Provimi Kliba AG, Gossau, Switzerland). All procedures were according to Swiss legislation and approved by the cantonal veterinary administration. Generation of cell lines and in vitro assays are further documented in Supplementary Materials and Methods online.

Gene expression analysis

Total RNA from melanoma cell lines and tumors was isolated using Trizol reagent (Thermo Fisher Scientific, Waltham, MA) and guanidinium/CsCl gradient, respectively, or by using the RNeasyMini kit (Qiagen, Venlo, Netherlands). One microgram of total RNA was used for cDNA synthesis using the Superscript III Reverse Transcription Kit (Invitrogen, Carlsbad, CA). Quantitative polymerase chain reaction assays were performed using SYBR green chemistry according to manufacturers' instructions (Applied Biosystems, Waltham, MA), or commercial Taqman probe for INHβA (Eurogentec, Liège, Belgium). PCR primer sequences are listed in Supplementary Table S1 online.

Cell cycle and Ki67 analysis

After treatment with 250 μg/ml doxycycline for 24, 48 or 72 hours in 6-well plates, cells were incubated with 10 μM 5-ethynyl-2′-deoxyuridine for 30 minutes and then trypsinized, washed with phosphate buffered saline, and fixed for 20 minutes with 4% paraformaldehyde, permeabilized with 0.5% Triton X-100 in phosphate buffered saline, and stained for 30 minutes with Alexa-647-coupled azide in the presence of copper sulfate and sodium ascorbate. Cells were then washed and stained with DAPI and analyzed using a CyAn ADP analyzer (Beckman Coulter, Brea, CA). For Ki67 immunostaining, tumors were dissociated into single cells in 0.02 mg/ml DNase I and 1 mg/ml collagenase mix (Sigma-Aldrich, St. Louis, MO) using a GentleMACS tissue octo dissociator (Miltenyi, Bergisch Gladbach, Germany). Dissociated cells were stained with live and dead blue dye (Life Technologies, Carlsbad, CA), and washed and labeled with antibodies against CD45-APC-Vio770 (Miltenyi, 130-105-463), CD31-BV605 (BD Biosciences, Franklin Lakes, NJ, 740356), and CD140a-PE (eBioscience, Waltham, MA, 12-1401-81) to exclude leukocytes, endothelial cells, and fibroblasts, respectively. After washing, cells were fixed and permeabilized using FoxP3 fix and perm buffer set (eBiosciences) and stained with eFluor 450-conjugated Ki67 antibodies (eBiosciences, 48-5698-80) using permeabilization buffer (eBiosciences). Samples were acquired using an LSRII cytometer (Becton Dickinson, Franklin Lakes, NJ).

Statistical analysis

All statistical analyses were performed using GraphPad Prism v6 software. Data were analyzed using Mann-Whitney (for nonparametric data), *t*-tests, and 1-way or 2-way analysis of variance with Bonferroni correction for parametric data. A *P*-value <0.05 was considered significant.

ORCID

Daniel B. Constam: http://orcid.org/0000-0002-6256-3891

CONFLICT OF INTEREST

The authors state no conflict of interest.

ACKNOWLEDGMENTS

We thank Dr Joerg Huelsken for the kind gift of lentiviral Gateway cloning vectors, Dr Malcom Whitman for HA-tagged human ALK4 cDNA, and Drs U. Koch, J. Faget, and M. De Palma for advice on FACS, and M. Langegger for culturing melanoma cells for zebrafish transplantations, and the EPFL School of Life Sciences technology cores and animal care facility. This work was supported by grants to DBC from the Swiss Cancer League (KLS—02487-08-2009 and the Swiss National Science foundation (31003A_156452).

SUPPLEMENTARY MATERIAL

Supplementary material is linked to the online version of the paper at www.jidonline.org, and at http://dx.doi.org/10.1016/j.jid.2017.07.845.

REFERENCES

Alanko T, Saksela O. Transforming growth factor beta1 induces apoptosis in normal melanocytes but not in nevus cells grown in type I collagen gel. J Invest Dermatol 2000;115:286–91.

Antsiferova M, Huber M, Meyer M, Piwko-Czuchra A, Ramadan T, Macleod AS, et al. Activin enhances skin tumourigenesis and malignant progression by inducing a pro-tumourigenic immune cell response. Nat Commun 2011;2:576.

Antsiferova M, Piwko-Czuchra A, Cangkrama M, Wietecha M, Sahin D, Birkner K, et al. Activin promotes skin carcinogenesis by attraction and reprogramming of macrophages. EMBO Mol Med 2017;9:27–45.

Bellomo C, Caja L, Moustakas A. Transforming growth factor beta as regulator of cancer stemness and metastasis. Br J Cancer 2016;115:761–9.

Breit S, Ashman K, Wilting J, Rossler J, Hatzi E, Fotsis T, et al. The N-myc oncogene in human neuroblastoma cells: down-regulation of an angiogenesis inhibitor identified as activin A. Cancer Res 2000;60:4596–601.

Caramel J, Papadogeorgakis E, Hill L, Browne Gareth J, Richard G, Wierinckx A, et al. A Switch in the expression of embryonic EMT-inducers drives the development of malignant melanoma. Cancer Cell 2013;24:466–80.

Chen W, Jin W, Hardegen N, Lei KJ, Li L, Marinos N, et al. Conversion of peripheral CD4+CD25− naive T cells to CD4+CD25+ regulatory T cells by TGF-beta induction of transcription factor Foxp3. J Exp Med 2003;198:1875–86.

Deli A, Kreidl E, Santifaller S, Trotter B, Seir K, Berger W, et al. Activins and activin antagonists in hepatocellular carcinoma. World J Gastroenterol 2008;14:1699–709.

Fearon K, Arends J, Baracos V. Understanding the mechanisms and treatment options in cancer cachexia. Nat Rev Clin Oncol 2013;10:90–9.

Fidler IJ. Selection of successive tumour lines for metastasis. Nat New Biol 1973;242:148–9.

Ghiringhelli F, Puig PE, Roux S, Parcellier A, Schmitt E, Solary E, et al. Tumor cells convert immature myeloid dendritic cells into TGF-beta-secreting cells inducing CD4+CD25+ regulatory T cell proliferation. J Exp Med 2005;202:919–29.

Gorelik L, Flavell RA. Immune-mediated eradication of tumors through the blockade of transforming growth factor-beta signaling in T cells. Nat Med 2001;7:1118–22.

Gritsman K, Zhang J, Cheng S, Heckscher E, Talbot WS, Schier AF. The EGF-CFC protein one-eyed pinhead is essential for nodal signaling. Cell 1999;97:121–32.

Hedger MP, Winnall WR, Phillips DJ, de Krester DM. The regulation and functions of Activin and Follistatin in inflammation and immunity. Vitam Horm 2011;85:255–97.

Heinz M, Niederleithner HL, Puujalka E, Soler-Cardona A, Grusch M, Pehamberger H, et al. Activin A is anti-lymphangiogenic in a melanoma mouse model. J Invest Dermatol 2015;135:212–21.

Hoda MA, Rozsas A, Lang E, Klikovits T, Lohinai Z, Torok S, et al. High circulating activin A level is associated with tumor progression and predicts poor prognosis in lung adenocarcinoma. Oncotarget 2016;7:13388–99.

Hoek KS, Eichhoff OM, Schlegel NC, Dobbeling U, Kobert N, Schaerer L, et al. In vivo switching of human melanoma cells between proliferative and invasive states. Cancer Res 2008;68:650–6.

Hoek KS, Schlegel NC, Brafford P, Sucker A, Ugurel S, Kumar R, et al. Metastatic potential of melanomas defined by specific gene expression profiles with no BRAF signature. Pigment Cell Res 2006;19:290–302.

Javelaud D, Delmas V, Moller M, Sextius P, Andre J, Menashi S, et al. Stable overexpression of Smad7 in human melanoma cells inhibits their tumorigenicity in vitro and in vivo. Oncogene 2005;24:7624–9.

Javelaud D, Mohammad KS, McKenna CR, Fournier P, Luciani F, Niewolna M, et al. Stable overexpression of Smad7 in human melanoma cells impairs bone metastasis. Cancer Res 2007;67:2317–24.

Kaneda H, Arao T, Matsumoto K, De Velasco MA, Tamura D, Aomatsu K, et al. Activin A inhibits vascular endothelial cell growth and suppresses tumour angiogenesis in gastric cancer. Br J Cancer 2011;105:1210–7.

Krneta J, Kroll J, Alves F, Prahst C, Sananbenesi F, Dullin C, et al. Dissociation of angiogenesis and tumorigenesis in follistatin- and activin-expressing tumors. Cancer Res 2006;66:5686–95.

Lau PK, Ascierto PA, McArthur G. Melanoma: the intersection of molecular targeted therapy and immune checkpoint inhibition. Curr Opin Immunol 2016;39:30–8.

Lewis Claire E, Harney Allison S, Pollard Jeffrey W. The multifaceted role of perivascular macrophages in tumors. Cancer Cell 2016;30:18–25.

Li Q, Kumar R, Underwood K, O'Connor AE, Loveland KL, Seehra JS, et al. Prevention of cachexia-like syndrome development and reduction of tumor progression in inhibin-deficient mice following administration of a chimeric activin receptor type II-murine Fc protein. Mol Hum Reprod 2007;13:675–83.

Lonardo E, Hermann PC, Mueller M-T, Huber S, Balic A, Miranda-Lorenzo I, et al. Nodal/Activin signaling drives self-renewal and tumorigenicity of pancreatic cancer stem cells and provides a target for combined drug therapy. Cell Stem Cell 2011;9:433–46.

Loomans HA, Andl CD. Intertwining of Activin A and TGFbeta signaling: dual roles in cancer progression and cancer cell invasion. Cancers 2014;7:70–91.

Perrot CY, Javelaud D, Mauviel A. Insights into the transforming growth factor-beta signaling pathway in cutaneous melanoma. Ann Dermatol 2013;25:135–44.

Pinner S, Jordan P, Sharrock K, Bazley L, Collinson L, Marais R, et al. Intravital imaging reveals transient changes in pigment production and Brn2 expression during metastatic melanoma dissemination. Cancer Res 2009;69:7969–77.

Qiu W, Tang SM, Lee S, Turk AT, Sireci AN, Qiu A, et al. Loss of Activin receptor type 1B accelerates development of intraductal papillary mucinous neoplasms in mice with activated KRAS. Gastroenterology 2016;150:218–28 e12.

Riker AI, Enkemann SA, Fodstad O, Liu S, Ren S, Morris C, et al. The gene expression profiles of primary and metastatic melanoma yields a transition point of tumor progression and metastasis. BMC Med Genom 2008;1:13.

Rodeck U, Melber K, Kath R, Menssen HD, Varello M, Atkinson B, et al. Constitutive expression of multiple growth factor genes by melanoma cells but not normal melanocytes. J Invest Dermatol 1991;97:20–6.

Rodeck U, Nishiyama T, Mauviel A. Independent regulation of growth and SMAD-mediated transcription by transforming growth factor beta in human melanoma cells. Cancer Res 1999;59:547–50.

Schatton T, Frank MH. Antitumor immunity and cancer stem cells. Ann NY Acad Sci 2009;1176:154–69.

Sozzani S, Musso T. The yin and yang of Activin A. Blood 2011;117:5013–5.

Stove C, Vanrobaeys F, Devreese B, Van Beeumen J, Mareel M, Bracke M. Melanoma cells secrete follistatin, an antagonist of activin-mediated growth inhibition. Oncogene 2004;23:5330–9.

Theologides A. Cancer cachexia. Cancer 1979;43(Suppl):2004–12.

Togashi Y, Kogita A, Sakamoto H, Hayashi H, Terashima M, de Velasco MA, et al. Activin signal promotes cancer progression and is involved in cachexia in a subset of pancreatic cancer. Cancer Lett 2015;356(Pt B):819–27.

Togashi Y, Sakamoto H, Hayashi H, Terashima M, de Velasco MA, Fujita Y, et al. Homozygous deletion of the activin A receptor, type IB gene is associated with an aggressive cancer phenotype in pancreatic cancer. Mol Cancer 2014;13:126.

Topczewska JM, Postovit LM, Margaryan NV, Sam A, Hess AR, Wheaton WW, et al. Embryonic and tumorigenic pathways converge via Nodal signaling: role in melanoma aggressiveness. Nat Med 2006;12:925–32.

Turk MJ, Guevara-Patino JA, Rizzuto GA, Engelhorn ME, Sakaguchi S, Houghton AN. Concomitant tumor immunity to a poorly immunogenic melanoma is prevented by regulatory T cells. J Exp Med 2004;200:771–82.

Van Belle P, Rodeck U, Nuamah I, Halpern AC, Elder DE. Melanoma-associated expression of transforming growth factor-beta isoforms. Am J Pathol 1996;148:1887–94.

Walton KL, Makanji Y, Harrison CA. New insights into the mechanisms of activin action and inhibition. Mol Cell Endocrinol 2011;359:2–12.

Widmer DS, Cheng PF, Eichhoff OM, Belloni BC, Zipser MC, Schlegel NC, et al. Systematic classification of melanoma cells by phenotype-specific gene expression mapping. Pigment Cell Melanoma Res 2012;25:343–53.

Wu S, Qi Y, Niu LM, Xie DX, Cui XL, Liu ZH. Activin A as a novel biomarker for colorectal adenocarcinoma in humans. Eur Rev Med Pharmacol Sci 2015;19:4371–8.

Yang G, Li Y, Nishimura EK, Xin H, Zhou A, Guo Y, et al. Inhibition of PAX3 by TGF-β modulates melanocyte viability. Mol Cell 2008;32:554–63.

Yin M, Soikkeli J, Jahkola T, Virolainen S, Saksela O, Holtta E. TGF-beta signaling, activated stromal fibroblasts, and cysteine cathepsins B and L drive the invasive growth of human melanoma cells. Am J Pathol 2012;181:2202–16.

Zhou X, Wang JL, Lu J, Song Y, Kwak KS, Jiao Q, et al. Reversal of cancer cachexia and muscle wasting by ActRIIB antagonism leads to prolonged survival. Cell 2010;142:531–43.

This work is licensed under a Creative Commons Attribution 4.0 International License. To view a copy of this license, visit http://creativecommons.org/licenses/by/4.0/